



Published in final edited form as:

J Cell Physiol. 2012 July ; 227(7): 2870–2879. doi:10.1002/jcp.23028.

Bone Morphogenetic Protein Receptor Type Ia Localization Causes Increased BMP2 Signaling in Mice Exhibiting Increased Peak Bone Mass Phenotype

Beth Bragdon^{1,2}, Jeremy Bonor¹, Kathryn L. Schultz³, Wesley G. Beamer³, Clifford J. Rosen⁴, and Anja Nohe^{1,*}

¹Department of Biological Sciences, University of Delaware, Newark, Delaware 19716 USA

²Department of Molecular and Biomedical Sciences, University of Maine, Orono, Maine 04469 USA

³The Jackson Laboratory, Bar Harbor, Maine 04609 USA

⁴Maine Medical Center Research Institute, Scarborough, Maine 04074 USA

Abstract

Bone Morphogenetic Protein 2 (BMP2) is a growth factor that initiates osteoblast differentiation. Recent studies show that BMP2 signaling regulates bone mineral density (BMD). BMP2 interacts with BMP receptor type Ia (BMPRIa) and type II receptor leading to the activation of the Smad signaling pathway. BMPRIa must shuttle between distinct plasma membrane domains, enriched of Caveolin-1 alpha and Caveolin-1 beta isoforms, and receptor activation occurs in these domains. Yet it remains unknown whether the molecular mechanism that regulates BMP2 signaling is driving mineralization and BMD. Therefore the B6.C3H-1-12 congenic mouse model with increased BMD and osteoblast mineralization was utilized in this study. Using the Family Image Correlation Spectroscopy, we determined if BMP2 led to a significant re-localization of BMPRIa to caveolae of the alpha/beta isoforms in bone marrow stromal cells (BMSCs) isolated from B6.C3H-1-12 mice compared to the C57BL/6J mice, which served as controls. The control, C57BL/6J mice, was selected due to only 4Mb of Chromosome 1 from the C3H/HeJ mouse was backcrossed to a C57BL/6J background. Using reporter gene assays, the B6.C3H-1-12 BMSCs responded to BMP2 with increased Smad activation. Furthermore disrupting caveolae reduced the BMP2-induced Smad signaling in BMSCs isolated from B6.C3H-1-12 and C57BL/6J. This study suggests for the first time a regulatory mechanism of BMPRIa signaling at the plasma membrane of BMSCs that 1) associated with genetic differences in the distal Chromosome 1 segment carried by the B6.C3H-1-12 congenic and 2) contributes to increase BMD of the B6.C3H-1-12 compared to the C57BL/6J control mice.

Keywords

Bone; Image Cross Correlation Spectroscopy; Membrane; Caveolae

Introduction

Bone Morphogenetic Protein 2 (BMP2) is a growth factor belonging to the TGF beta superfamily. BMP2 directs differentiation of bone marrow stromal cells (BMSCs) into

*To whom correspondence should be addressed at Department of Biology, University of Delaware, Newark, DE, 19716, USA, Phone: (302) 831-2959, Fax: (302) 831-2281, anjanohe@udel.edu.

osteoblasts, adipocytes, and chondrocytes (Bragdon et al., 2011; Chiellini et al., 2008; Crockett et al., 2011; Hata et al., 2003; Moerman et al., 2004; Ponce et al., 2008; Sottile and Seuwen, 2000). Mouse models have shown BMP2 and its potent receptor BMPR receptor type Ia (BMPRIa) regulate bone modeling and remodeling, although the conclusions are perplexing (Kamiya et al., 2008; Kaps et al., 2004; Mishina et al., 2004; Ovchinnikov et al., 2006; Yeh et al., 2000). The disruption of BMP signaling through a conditional knockout of BMPRIa in mature osteoblasts reduced bone mass at 3 months while it was increased at 10 months (Mishina et al., 2004). When the disruption of BMP signaling through BMPRIa was induced and affected pre-osteoblasts and mature osteoblasts, there was a decrease in bone formation and mineral apposition rate (Kamiya et al., 2008). Furthermore, conditional knockouts of BMPRIa in limb bud mesenchyme showed severe limb defects (Ovchinnikov et al., 2006). Specifically for BMSCs isolated from rat calvaria showed BMPRIa and BMPRII increased expression with BMP7, no changes were observed with BMPRIb during different stages of osteoblasts (days 3, 6, and 9) (Yeh et al., 2000). Further implanted collagen sponges with BMP2 into rats formed ectopic bone. During the process of ectopic bone formation the mRNA and protein expression increased for BMPRIa and BMPRII but again there was no significant expression detected with mRNA or protein for BMPRIb (Nakamura et al., 2003). These studies suggest that BMPRIa and not BMPRIb is activating osteoblast differentiation. The BMP2 signaling response through BMPRIa impacts bone yet the specific role is unclear.

BMP2 signals through serine threonine kinase receptors of the type-I and type-II (Bragdon et al., 2011; Chang et al., 2002; Hartung et al., 2006; Mishra and Marshall, 2006). Specific BMP receptors, BMPRIa and BMPR receptor type II (BMPRII), aggregate dependent on their association with membrane proteins and their own inherent properties allowing for signaling to be regulated on the membrane surface (Hartung et al., 2006; Nohe et al., 2004a; Nohe et al., 2004b). The plasma membrane is heterogeneous consisting of lipids, cholesterol and proteins. Within the surface are areas of aggregation called membrane domains such as clathrin coated pits, caveolae and lipid rafts (Lajoie et al., 2009; Semrau and Schmidt, 2009). BMPRIa is co-localized and activated within caveolae (Bonor et al.,; Bragdon et al., 2009; Hartung et al., 2006; Nohe et al., 2006; Nohe et al., 2004b). Caveolae are small, flask shaped invaginations in the cell membrane where Caveolin-1 (Cav1) is a marker. Two isoforms of Cav1 have been identified, Cav1 alpha (Cav1 α) and Cav1 beta (Cav1 β). Currently only two caveolae populations have been observed, one enriched in isoforms of Cav1 α and β (Cav1 $\alpha\beta$) and the second enriched in only Cav1 β (Fujimoto et al., 2000). BMPRIa localized to caveolae preferentially binds to BMP2. BMP2 stimulation causes the BMPRIa co-localization to change, inferring a movement of BMPRIa from one location to another at the cell surface also known as receptor shuttling (Nohe et al., 2005). BMPRIa shuttles out of Cav1 β caveolae into Cav1 $\alpha\beta$ caveolae to activate Smad signaling (Nohe et al., 2003; Nohe et al., 2005). Caveolae are also sites where the activation of BMPRIa occurs (Bonor et al., Accepted). BMPRIa is phosphorylated and activated by BMPRII which in turn initiates the Smad signaling cascade. Activation of *RUNX2* (also known as *Cbfa1*), which is critical for osteoblast differentiation, is downstream of Smad signaling (Lee et al., 2000; Zhang et al., 2000).

Although BMP2 signaling is dependent on BMPRIa aggregation and shuttling between distinct plasma membrane domains (Nohe et al., 2003; Nohe et al., 2005; Nohe and Petersen, 2004a), the importance of receptor aggregation and shuttling on BMD still needs to be determined. The congenic mouse model, B6.C3H-1-12, which has increased BMD was utilized to identify molecular dynamic of BMPRIa in the plasma membrane of primary BMSCs. B6.C3H-1-12 mice strain was developed to study the genetic regulation of BMD Chromosome 1 (Chr1). The B6.C3H-1-12 congenic carries approximately 4 Mb of C3H/HeJ (175 – 179 Mb) on a C57BL/6J background strain (genetic haplotype map showing

chromosomal regions represented in the B6.C3H-1-12 subline) (Beamer et al., 2007). This allows for an access to the effects of the C3H/HeJ alleles in this segment of Chr1. The C57BL/6J mice were chosen as a control since only 4Mb of Chr1 from the C3H/HeJ mouse was backcrossed to a C57BL/6J background. Here we show using the Family Image Correlation Spectroscopy (FICS) BMP2 stimulation induced an aggregation of caveolae in BMSCs isolated from the B6.C3H-1-12 compared to C57BL/6J mice. FICS is a family of tools including image correlation spectroscopy (ICS) and image cross correlation spectroscopy (ICCS). ICS is used to determine the cluster density of a protein or the number of protein clusters per unit area while ICCS quantifies the percent co-localization between two proteins in the plasma membrane (Nohe and Petersen, 2004a; Nohe and Petersen, 2004b). BMPRIa significantly re-localized with caveolae of the Cav1 $\alpha\beta$ isoform in BMSCs isolated from B6.C3H-1-12 mice compared to C57BL/6J (Summarized in Figure 1). Smad signaling and mineralization was increased with BMP2 stimulation in the B6.C3H-1-12 BMSCs. Finally disrupting caveolae reduced the BMP2-induced Smad signaling in BMSCs isolated from B6.C3H-1-12 and C57BL/6J mice. Our results demonstrates the shuttling of BMPRIa at the cell surface enhances BMP2 induced Smad signaling. Furthermore, BMPRIa co-localization with caveolae is crucial for that signaling. For the first time a regulatory mechanism of BMPRIa signaling at the plasma membrane of BMSCs is linked to mineralization and BMD associated with the presence of C3H alleles within the distal Chr 1 region of the B6.C3H-1-12 congenic mice.

Materials and Methods

Materials

Recombinant BMP-2 was obtained from R&D Systems (Minneapolis, MN). The polyclonal goat anti-sera against the BMP receptor BMPRIa, the Alexa 546 red X conjugated donkey anti-goat antibody and Alexa 488 goat anti mouse antibody, mouse antisera against Caveolin alpha and alpha/beta were from Santa Cruz (Santa Cruz, CA). Mice strains C57BL/6J and B6.C3H-1-12 were both housed at The Jackson Laboratory and the University of Delaware and protocols were approved by the appropriate Institutional Animal Care and Use Committee (IACUC).

Isolation of BMSCs

BMSCs were collected from the tibia and femur of 8 week old females of age matched B6.C3H-1-12 congenic mice and C57BL/6J as controls. The C57BL/6J mice were chosen as a control since only 4Mb of Chr1 from the C3H/HeJ mouse was backcrossed to a C57BL/6J background. Mice were sacrificed with use of CO₂ and hind limbs were removed. In sterile conditions, tibia and femur were cleaned of fat and muscle, and the BMSCs were isolated by removing the epiphyses and flushing the marrow from the bones using a 25 gauge needle and plating media. Cell suspension was then passed through a 70 μ m filter and counted and plated to 1.0×10^6 cells on glass cover slips in 60 mm dishes for imaging or 2.0×10^7 cells in 35 mm dish for reporter gene assays or 24 well plates for von Kossa staining. Cells were isolated and cultured in minimum essential medium alpha media supplemented with 10% FBS and 1% Penicillin/Streptomycin.

Reporter Gene Assay

BMSCs were grown in 60 mm dishes for 10 days, then serum starved overnight. Cells were transfected with 2 μ g reporter plasmid encoding pSBE (Smad Binding Element) or Cbfa1, and 2 μ g pRL-luc plasmids for normalization. Cells were transfected with Lipofectamine 2000 from Invitrogen (Carlsbad, CA) according to the manufacturer's instructions. Four hours after transfection, cells were stimulated with 40 nM BMP2 or solution vehicle stimulated. After 12 hours of incubation, cells were washed with PBS, lysed and the

luciferase activity was measured using a dual luciferase assay system (Promega, Madison, WI).

Immunofluorescence labeling of cell surface receptors

To measure the distribution of the BMPRIa and Caveolin on the cell surface, we employed confocal fluorescence imaging measurements. BMSCs were cultured on 22 mm glass cover slips for 10 days. Cells were serum starved overnight then either stimulated or not with 40nM of BMP2. Cells were fixed by the acetone/methanol method (Brown and Petersen, 1998). Cells were incubated for 30 min with 3% BSA to minimize non-specific binding. Cells were incubated with polyclonal goat anti-sera recognizing BMPRIa according to manufacturer's protocol. After the cells were washed three times with PBS, they were incubated again with the corresponding secondary donkey anti-goat at a concentration of 20 µg/mL. Cells were labeled again with either anti-mouse Caveolin1 alpha or Caveolin1 alpha/beta for 20 min and washed three times. Lastly cells were labeled with the secondary anti-mouse, washed and cover slips were mounted with Airvol (Nohe et al., 2005).

Image Correlation Spectroscopy and Image Cross Correlation Spectroscopy

Image correlation spectroscopy (ICS) was the technique used to study the distribution and localization of the BMPRs. High resolution and high magnification images were collected by confocal microscopy. ICS involves autocorrelation analysis of the intensity fluctuations within these confocal images, in this case from immunofluorescent labelled proteins (Nohe and Petersen, 2004a; Nohe and Petersen, 2004b; Nohe and Petersen, 2007). From this, the cluster density (CD) was calculated from equation 1 (Nohe and Petersen, 2007).

$$CD = \frac{1}{g(0,0)\pi w^2} = \frac{\bar{N}_p}{\pi w^2} \quad (\text{Eq 1})$$

Image cross-correlation spectroscopy (ICCS) was the tool used to quantify the extent of co-localization between two proteins. It is based upon the autocorrelation and CD from ICS. The autocorrelation is calculated for each image separately and then the cross-correlation function is calculated from the two images. This represents the average density of clusters in which both proteins localize together. The fraction of one protein co-localizing with the other can be calculated (Nohe and Petersen, 2004b; Nohe and Petersen, 2007). Figure 2 shows a sample image, autocorrelation, and cross correlation functions for BMSCs isolated from the C57BL/6J labelled for A) BMPRIa and B) Cav1 α.

It is important to note that there are only two antibodies available for Cav1. There is antibody for both Cav1 αβ and Cav1 β, known in this paper as Cav1 total. A second antibody, Cav1 α, labels only Cav1 α. Since Cav1 α is only found in Cav1 αβ caveolae this antibody is used for labeling Cav1 αβ caveolae (Fujimoto et al., 2000). There is no antibody specifically available for Cav1 β, therefore we must use calculations based on the labeling of Cav1 total and Cav1 α to identify the dynamics of Cav1 β. We only use one antibody for the labeling of total BMPRIa at the cell surface.

Using the calculations of ICCS the amount of total BMPRIa co-localized with labeled Cav1 α is equal to the amount of BMPRIa co-localized with caveolae enriched with Cav1 αβ. And the total amount of BMPRIa co-localized with Cav1 total is the total amount of BMPRIa co-localized with total amount of caveolae. Since there is only one antibody for BMPRIa and labeling is saturated by this antibody, we can assume the total amount of BMPRIa labeled is the same between Cav1 α and Cav1 total labeling. We can therefore infer that the percentage of BMPRIa co-localized with caveolae enriched with Cav1 β (BMPRIa_{Cav1 β}) is equal to

the difference between the percentage of BMPRIa co-localized with Cav1 total (BMPRIa_{Cav1 total}) and Cav1 α (BMPRIa_{Cav1 α}) shown in (Eq2).

$$\text{BMPRIa}_{\text{Cav1 } \beta} = \text{BMPRIa}_{\text{Cav1 total}} - \text{BMPRIa}_{\text{Cav1 } \alpha} \quad \text{Eq2}$$

We cannot determine the percent of Cav1 β co-localized with BMPRIa in the similar manner. This is due to the fact there are two different antibodies used for caveolae labeling. The total amount of labeled Cav1 α will not equal the total amount of caveolae and therefore two populations are labeled. These percentages cannot be used in an additive manner. The co-localization of labeled Cav1 α with BMPRIa is a true representative for caveolae enriched with Cav1 $\alpha\beta$. The co-localization of Cav1 total is the average percentage of Cav1 $\alpha\beta$ enriched caveolae with BMPRIa (labeled for Cav1 α) and Cav1 β enriched caveolae with BMPRIa (Eq 3), assuming the number of Cav1 $\alpha\beta$ is similar to Cav1 β , as shown in (Fujimoto et al., 2000). We can then calculate the percentage of Cav1 β enriched domains co-localized with BMPRIa (Eq 4).

$$\text{Cav1 total}_{\text{BMPRIa}} = (\text{Cav1 } \alpha_{\text{BMPRIa}} + \text{Cav1 } \beta_{\text{BMPRIa}}) / 2 \quad \text{Eq3}$$

$$\text{Cav1 } \beta_{\text{BMPRIa}} = 2\text{Cav1 total}_{\text{BMPRIa}} - \text{Cav1 } \alpha_{\text{BMPRIa}} \quad \text{Eq4}$$

von Kossa staining for mineral

Isolated BMSCs were cultured in 24 well plates for 10 days and serum starved overnight prior to stimulation. Von Kossa was performed and quantified as described previously with the exception that cells were only treated with BMP2 (40nM) for 12 days and 15 random images per well per treatment was used for the quantification (Bragdon et al.). Non-stimulated cells served as controls. BMP2 treatments were normalized to corresponding control.

Statistics

Mean values and standard error of the mean (SEM) were calculated from the raw data at the 95% confidence level. SEM was used as error bars. Experiments were performed three times for reporter gene assays and von Kossa staining, and twice for FICS. Each experiment consisted of 3–5 eight week old female mice. For ICS measurements, 40 images of individual cells were taken per experiment. Outliers that were more than three standard deviations from the mean were removed and percent of co-localization was set to 100% when calculations showed over 100%. Student t tests were performed for between treatments for C57BL/6J or B6.C3H-1-12. ANOVA followed by Tukey's HSD test was performed for reporter gene assays for the knockdown of Cav1 with the use of siRNA against Cav1.

Results

No change in aggregation of BMPRIa on the cell surface of BMSCs isolated from B6.C3H-1-12 mice in response to BMP2

BMP2 signaling regulates osteoblast differentiation and drives BMD. Critical for BMP2 signaling is BMPRIa aggregation on the plasma membrane (Nohe et al., 2003; Nohe et al., 2005; Nohe and Petersen, 2004a). Yet it is unknown whether BMPRIa aggregation on the plasma membrane of BMSCs regulates BMP2 signaling and affects mineralization and BMD. Therefore the cluster density was first determined using the B6.C3H-1-12 mouse

model, which has increased number of osteoprogenitors and BMD. Aggregation is determined by using confocal images of fluorescently labeling proteins and applying ICS to quantify the cluster density (CD) of the protein. ICS is unique tool to study the aggregation and clustering of proteins in the plasma membrane (Nohe and Petersen, 2004b). CD is the number of protein clusters per unit area at the cell surface (μm^2). A decrease in CD suggests there is an aggregation of clusters reducing the number of clusters present. An increase in CD demonstrates there is a possible dispersion of the clusters. These conclusions hold true if there is no change in the intensity of the protein at the plasma membrane showing the decrease or increase in CD is not due to a change in the number of proteins present. For BMPRIa signaling in A431 cells it was shown that the BMPRIa CD must decrease resulting in aggregation for Smad activation to occur.

The CD of BMPRIa was determined for B6.C3H-1-12 compared to C57BL/6J BMSCs as control. The C57BL/6J mice were chosen as a control since only 4Mb of Chr1 from the C3H/HeJ mouse was backcrossed to a C57BL/6J background. After isolation of BMSCs from B6.C3H-1-12 and C57BL/6J mice the cells were fixed and labelled for BMPRIa. High magnification images of flat regions of the cell membrane were collected and analyzed by ICS. As Figure 3A shows BMP2 stimulation led to a significant decrease in the CD in BMSCs isolated from C57BL/6J. The cluster density of BMPRIa in BMSCs isolated from B6.C3H-1-12 did not respond to BMP2 stimulation, it already showed aggregation of receptor clusters. The results are summarized if figure 3B. The C57BL/6J results are similar to the previous ICS results (Nohe et al., 2003) while in the 1-12 the data suggest BMPRIa is already aggregated.

BMP2 stimulation led to a decrease in aggregation of Caveolin-1 α domains in BMSCs isolated from B6.C3H-1-12 mice

In the C57BL/6J BMSCs, the number of CD for BMPRIa significantly decreased with BMP2 stimulation showing aggregation at the cell surface, while receptors in B6.C3H-1-12 were already aggregated. Recent data showed that BMP2 binds with high affinity to receptors localized in caveolae (Bonor et al., Accepted). Additionally BMP receptors shuttle between caveolae isoforms on the plasma membrane (Nohe et al., 2003; Nohe et al., 2005). Therefore we determined the aggregation or CD of caveolae at the plasma membrane surface of BMSCs isolated from C57BL/6J and B6.C3H-1-12 mice in response to BMP2 with the use of ICS. The CD for Cav1 shows the number of Cav1 clusters per μm^2 . It allows for a description of the dynamics for caveolae.

Figure 4A shows there is a trend of increased CD of Cav1 α on the cell surface of BMSCs isolated from C57BL/6J and a significant decrease for the B6.C3H-1-12 mice ($p < 0.05$) in response to BMP2. Furthermore, the CD of Cav1 total did not change at the cell surface of BMSCs of the C57BL/6J with BMP2 stimulation (Figure 4C). Labelled Cav1 total, which includes Cav1 $\alpha\beta$ and Cav1 β , showed CD of the B6.C3H-1-12 significantly increased from a normalized CD of 1.07 to 1.3 with BMP2 stimulation. The cell surfaces of BMSCs from C57BL/6J did not significantly change while the B6.C3H-1-12 did respond to BMP2 stimulation. This data indicates that the number of caveolae enriched with Cav1 α isoforms slightly increased and a few of the Cav1 β disappears in the C57BL/6J while in B6.C3H-1-12 cells the caveolae of Cav1 α are reduced at the cell surface and Cav1 β appear in response to BMP2 stimulation. The results are summarized in a diagram in figure 4B.

Increased BMPRIa shuttling to Cav1 α enriched caveolae in the B6.C3H-1-12

We previously found that BMP2 bound to receptors in caveolae and using Image Cross Correlation Spectroscopy (ICCS) shuttles between caveolae isoforms for signaling (Bonor et al., Accepted; Nohe et al., 2004b; Nohe et al., 2003; Nohe et al., 2005). ICCS is novel tool to

study the co-localization of two proteins in the plasma membrane (Nohe and Petersen, 2004a). Since during BMP2 stimulation, the aggregation of BMPRIa is altered in B6.C3H-1-12 while the aggregation of caveolae is changed we next investigated whether BMPRIa shuttles between caveolae isoforms.

Figure 5 shows that 53% of BMPRIa co-localized with labelled Cav1 α and 49% co-localized with labelled Cav1 total in the BMSCs isolated from C57BL/6J mice. This indicates a non-significant amount of BMPRIa is co-localized with Cav1 β (Figure 5). BMP-2 stimulation caused no significant change for the co-localization of BMPRIa with labelled Cav1 total or Cav1 α . On the other hand, the response to BMP2 was determined by BMSCs isolated from B6.C3H-1-12 (Figure 5). 44% of BMPRIa co-localized with labelled Cav1 α and 59% co-localized with labelled Cav1 total in the B6.C3H-1-12 this is increased compared to the C57BL/6J. There was approximately 15% of BMPRIa co-localized with Cav1 β (Figure 5). BMP2 stimulation led to a significant increase to 52% of BMPRIa co-localizing to label Cav1 α and only a trend of decreasing amount of BMPRIa co-localizing with labelled Cav1 total. This indicates the 15% co-localized to Cav1 β shuttled to Cav1 α . This migration of BMPRIa out of Cav1 β was only observed in B6.C3H-1-12 cells and there was increased BMPRIa co-localized with caveolae.

Caveolin-1 isoforms show an increased co-localization with BMPRIa in BMSCs isolated B6.C3H-1-12 mice

BMPRIa at the cell surface of BMSCs localized to caveolae for both the C57BL/6J and B6.C3H-1-12 mice, with more co-localization in the B6.C3H-1-12. BMP2 response in the B6.C3H-1-12 resulted in the shuttling of BMPRIa from the Cav1 β to Cav1 α while there was no movement of BMPRIa in the BMSCs isolated from the C57BL/6J mice. Yet with BMP2 stimulation there are more caveolae domains present at the cell surface for the B6.C3H-1-12 cells. Therefore the percent of caveolae containing BMPRIa was determined for C57BL/6J and B6.C3H-1-12 cells either non-stimulated or stimulated with BMP2. The analyses of labelled BMSCs for BMPRIa and Cav1 α or Cav1 total showed 66% of labelled Cav1 α and 69% of labelled Cav1 total co-localized with BMPRIa, showing about 72% of Cav1 β contain BMPRIa (Figure 6). BMP2 stimulation did not lead to a significant increase of labelled Cav1 α and labelled Cav1 total co-localizing with BMPRIa.

In the B6.C3H-1-12 mice, 60% of labelled Cav1 α and 80% of labelled Cav1 total co-localized with BMPRIa (Figure 6). It indicates approximately all (100%) of Cav1 β co-localized with BMPRIa (Figure 6). The addition of BMP2 did not yield significant change for labelled Cav1 α co-localizing with BMPRIa, but there was a significant decrease in the co-localization between labelled Cav1 total and BMPRIa. This indicates a decrease in the co-localization of Cav1 β with BMPRIa (Figure 6).

Smad signaling is regulated by caveolae

Cultured BMSCs isolated from C57BL/6J and B6.C3H-1-12 were transfected with a reporter plasmid encoding pSBE (Smad Binding Element) and pRL-uc for normalization; cells were either stimulated or not. As figure 7A shows BMP2 stimulation significantly increased Smad signaling for both C57BL/6J and B6.C3H-1-12 BMSCs. In the B6.C3H-1-12 isolated BMSCs the BMP2 induced Smad signaling increase was 3 fold compared to the 1.6 fold increase in the C57BL/6J BMSCs.

We also quantified Smad signaling with the knockdown of Cav1 by siRNA to determine a relationship between caveolae and Smad signal. Knockdown of Cav1 in the absence of BMP2 did not alter Smad signaling from C57BL/6J. The addition of BMP2 did not increase Smad signaling that was observed with endogenous Cav1 (Figure 7B). The knockdown of

Cav1 in B6.C3H-1-12 induced a significant increase in Smad signaling in the absence of exogenous BMP2. The addition of BMP2 with the knockdown of Cav1 did not induce a Smad signal similar as to what was observed in C57BL/6J.

Downstream of BMP2-Smad signaling is Cbfa1 and it is involved with osteoblast differentiation. Since osteoblasts isolated from B6.C3H-1-12 are more active than C57BL/6J, we used a reporter plasmid for Cbfa1 to determine whether BMSCs from B6.C3H-1-12 are more reactive to BMP2 compared to C57BL/6J mice. In the absence of BMP2, there was a significant 1.4 fold increase of Cbfa1 activity in the B6.C3H-1-12 BMSCs compared to C57BL/6J (Figure 7C). Interestingly BMP2 stimulation showed a slight but non-significant decrease in Cbfa1 activity for C57BL/6J (1 to 0.7) and a significant decreased for B6.C3H-1-12 (1.4 to 0.5).

BMP2 induced increased mineralization in the B6.C3H-1-12 cells

The BMP2-induced Smad pathway can drive osteoblast differentiation and mineralization. BMP2 induced Smad signaling in BMSCs isolated from the C57BL/6J and B6.C3H-1-12 mice with the response in the B6.C3H-1-12 being robust. Therefore we quantified the BMP2 induced mineralization of BMSCs in vitro by von Kossa staining. Images of stained cells were taken of the mineralization and quantified using ImageJ.

The area of mineralization was significantly increased with BMP2 treatment for both BMSCs isolated from the C57BL/6J and B6.C3H-1-12 mice (Figure 8). The response observed with the B6.C3H-1-12 mice was increased compared to the C57BL/6J. This is similar to the activation of the Smad pathway measured by SBE reporter. The BMSCs isolated from the B6.C3H-1-12 cells have increased receptor shuttling at the cell surface, Smad signaling, and mineralization compared to the C57BL/6J.

Discussion

The plasma membrane is a very heterogeneous environment consisting of lipids, cholesterol and proteins. Within the surface are areas of aggregation called membrane domains such as clathrin coated pits, caveolae and lipid rafts (Lajoie et al., 2009; Semrau and Schmidt, 2009). BMP receptors co-localize to these domains for various functions including signaling, endocytosis, and receptor turn over (Di Guglielmo et al., 2003; Nohe et al., 2005; Razani et al., 2001; Sieczkarski and Whittaker, 2002; Thomas and Smart, 2008). In this paper the membrane dynamics and activation of signaling pathways of BMSCs isolated from two mouse strains, C57BL/6J and the congenic B6.C3H-1-12 (results are summarized in Figure 1) were probed. The C57BL/6J mouse was used as the control since the B6.C3H-1-12 congenic was developed by back crossing 4Mb of Chr1 from the C3H/HeJ mice onto the C57BL/6J background. The BMD of the C57BL/6J mice has been shown to be low compared to other mouse strains (Judex et al., 2002).

BMP2 is a key growth factor driving osteoblast differentiation of BMSCs to osteoblasts and in vivo studies have linked BMP2 to BMD. A limb site specific inactivation of BMP2 (using the Prx1 Cre) in mice led to bilateral fractures at sites with decreased BMD. It was suggested the fractures were due to low BMD and architecture, due to the heterozygous mice demonstrated an intermediate expression of BMP2 and BMD although there were no fractures present (Tsuji et al., 2006). Disruption of BMP signaling through BMPRIa in mature mouse osteoblasts showed decreased bone mass (BV/TV) at 3 months, yet increased bone mass at 10 months, suggesting aging also influences BMPRIa signaling (Mishina et al., 2004). When the disruption of BMP signaling through BMPRIa was inducible and under a type I collagen promoter affecting pre-osteoblasts and mature osteoblasts, there was an increase in bone mass and BMD at 22 weeks while there was a decrease in bone formation

(BFR/BS) and mineral apposition rate (Kamiya et al., 2008). These results suggest BMPRIa regulates BMD specifically within the osteoblast lineage and is dependent upon age and the stage of differentiation of the osteoblast. Our study utilizes eight week old female mice before they reach their peak bone mass (Beamer et al., 1996). BMPRIa is used because it is thought to be responsible for the initiation of osteogenic development in cell lines and BMSCs (Kaps et al., 2004; Nakamura et al., 2003; Wang et al., 2010; Yeh et al., 2000), there is a possibility that BMPRIb contributes to Smad signaling (Skillington et al., 2002).

Using ICS we were able to calculate the CD for the two caveolae populations and BMPRIa on BMSCs from C57BL/6J and B6.C3H-1-12. The data suggests that for the B6.C3H-1-12 BMSC surface the caveolae enriched with Cav1 β disperse creating more caveolae while there is an aggregation of Cav1 $\alpha\beta$ enriched caveolae. The non-significant change in CD for caveolae in the C57BL/6J was surprising since an aggregation of Cav1 β enriched caveolae was observed in the A431 cell line (Nohe et al., 2004b). The BMPRIa clusters did aggregate in the C57BL/6J cells, as was predicted by previous results (Nohe et al., 2004b; Nohe et al., 2003; Nohe et al., 2005).

BMPRIa and BMPRII localize to caveolae enriched with Cav1 $\alpha\beta$ (here termed Cav1 α) and Cav1 β . BMPRIa shuttle from Cav1 β enriched caveolae upon BMP2 stimulation to Cav1 $\alpha\beta$ caveolae and clathrin coated pits at the cell surface (Bragdon et al., 2009; Nohe et al., 2004b; Nohe et al., 2005), though it is the BMPRIa localized to caveolae that interact with BMP2 and become activated for Smad signaling (Bonor et al., Accepted). Shuttling between caveolae of the isoforms was crucial for the activation of Smad signaling by BMP2 (Nohe et al., 2004b; Nohe et al., 2003; Nohe et al., 2005; Nohe and Petersen, 2004b). The amount of BMPRIa co-localized to Cav1 β caveolae was non-significant and the majority of BMPRIa (55%) co-localized with Cav1 α enriched caveolae. Furthermore, BMP2 stimulation did not lead to a significant change in the co-localization of BMPRIa with caveolae. In the B6.C3H-1-12 cells there was an increased amount of BMPRIa localized to Cav1 α enriched caveolae as well as Cav1 β enriched caveolae. BMP2 initiated BMPRIa to shuttle from Cav1 β caveolae to Cav1 α caveolae, which is similar to A431 cells. The shuttling of BMPRIa from Cav1 β caveolae to Cav1 α caveolae may be key for increased BMP2 signaling and BMD.

BMP2 activation of the Smad pathway is dependent upon the shuttling of BMPRIa from Cav1 β to Cav1 α caveolae due to Cav1 β being inhibitory to signaling (Nohe et al., 2003; Nohe et al., 2005). We investigated whether the B6.C3H-1-12 cells respond differently with BMP2 compared to C57BL/6J due to the shuttling of BMPRIa at the cell surface of the B6.C3H-1-12. BMP2 activated the Smad pathway in C57BL/6J and B6.C3H-1-12 cells, although the increase in Smad signaling of B6.C3H-1-12 was increased compared to the C57BL/6J response. The B6.C3H-1-12 BMSCs are more reactive to BMP2 and could increase the osteoblastic activity and number of progenitors. The mineralization stained by von Kossa showed similar results where the B6.C3H-1-12 cells showed increased mineralization in response to BMP2 compared to the C57BL/6J reaction to BMP2. This increase in activity in the B6.C3H-1-12 cells could be due to BMPRIa utilization of caveolae compared to C57BL/6J where BMPRIa is stagnant at the cell surface.

When caveolae were disrupted by knocking down Cav1 there was a loss of BMP2 response in C57BL/6J and B6.C3H-1-12 cells. In the absence of BMP2 the knockdown of Cav1 actually induced a Smad response in only the B6.C3H-1-12 cells. The loss of BMP2 response in both C57BL/6J and B6.C3H-1-12 indicate caveolae may be needed for Smad signaling to occur with BMP2 stimulation, since BMPRIa is localized to Cav1 α caveolae for both C57BL/6J and B6.C3H-1-12 cells. Interestingly the loss of caveolae in B6.C3H-1-12 induced Smad signaling independent of exogenous BMP2. This could be due

to Cav1 β interacting with BMPRII and inhibiting the activation of BMPRIa, thus the loss of Cav1 would no longer negatively regulate BMP receptor activation and Smad signaling. Also the dynamics and distribution of BMPRII are unknown for these cell types, since BMPRII is the BMP receptor that directly interacts with Cav1 β .

Downstream of Smad signaling is *Cbfa1* which is needed for osteoblast differentiation (Lee et al., 2000). The activation levels of Cbfa1 activity was increased in B6.C3H-1-12 compared to C57BL/6J cells at basal levels. This could be contributing to the increase osteoblastic progenitors and activity, but it is independent of Smad signaling, since the basal levels of Smad signaling for C57BL/6J and B6.C3H-1-12 were similar. The addition of BMP2 did not increase the activation of Cbfa1. The response time to see an increase in Cbfa1 by BMP2 could take longer than the 18 hours required for the reporter gene assays performance. This is supported by the increased mineralization of the BMSCs by BMP2. Although 18 hours of BMP2 stimulation reduced the activity of a crucial factor for osteoblast differentiation, Cbfa1, in BMSCs isolated from the C57BL/6J and B6.C3H-1-12 mice these cells when stimulated with BMP2 for 12 days significantly increased mineralization.

Our results showed: 1) BMP2 stimulation led Cav1 β caveolae to aggregate and Cav1 $\alpha\beta$ caveolae to disperse in the B6.C3H-1-12 BMSCs, while no change was observed with the C57BL/6J cells, 2) BMPRIa aggregates in the C57BL/6J with BMP2 stimulation, 3) BMPRIa shuttles out of Cav1 β caveolae and into Cav1 α caveolae in the B6.C3H-1-12 cells, 4) the B6.C3H-1-12 BMSCs are more reactive with Smad signaling by BMP2 stimulation, and 5) BMP2 induced mineralization is increased in the BMSCs of the B6.C3H-1-12 compared to C57BL/6J. These results suggest BMPRIa shuttling and co-localization with caveolae is crucial for BMP2 induced Smad signaling and mineralization. The isolated BMSCs from the B6.C3H-1-12 mice showed increased BMPRIa shuttling while BMSCs from the low BMD (C57BL/6J) demonstrated decreased receptor shuttling. Changes in BMPRIa shuttling and co-localization with caveolae of BMSCs can lead to changes in the response to BMP2-induced Smad pathway and enhanced bone mineralization associated with C3H alleles in distal Chr1 of the B6.C3H-1-12 congenic mice.

Acknowledgments

Grants:

Contract Grant Sponsor: National Institute of Health Contract Grant Number: RO1 AR043618

Contract Grant Sponsor: Startup University of Delaware Contract Grant Number: N/A

We the authors would like to thank Sue Seta, Shayamala Thinakaran, Lindsay Horton, Jane Maynard, and Harold Coumbs III for their assistance with the maintenance of the mice colony and isolation of BMSCs and Alex D'Angelo for his assistance with ICCS.

References

- Beamer WG, Donahue LR, Rosen CJ, Baylink DJ. Genetic variability in adult bone density among inbred strains of mice. *Bone*. 1996; 18(5):397–403. [PubMed: 8739896]
- Beamer WG, Shultz KL, Ackert-Bicknell CL, Horton LG, Delahunty KM, Coombs HF 3rd, Donahue LR, Canalis E, Rosen CJ. Genetic dissection of mouse distal chromosome 1 reveals three linked BMD QTLs with sex-dependent regulation of bone phenotypes. *J Bone Miner Res*. 2007; 22(8): 1187–1196.
- Bonor J, Adams EL, Bragdon B, Moseychuk O, Czymmek KJ, Nohe A. Initiation of BMP2 Signaling in Domains on the Plasma Membrane. *Journal of Cellular Physiology*. Accepted.

- Bragdon B, Moseychuk O, Saldanha S, King D, Julian J, Nohe A. Bone morphogenetic proteins: a critical review. *Cell Signal*. 2011; 23(4):609–620. [PubMed: 20959140]
- Bragdon B, Thinakaran S, Bonor J, Underhill TM, Petersen NO, Nohe A. FRET reveals novel protein-receptor interaction of bone morphogenetic proteins receptors and adaptor protein 2 at the cell surface. *Biophys J*. 2009; 97(5):1428–1435. [PubMed: 19720031]
- Bragdon B, Thinakaran S, Moseychuk O, King D, Young K, Litchfield DW, Petersen NO, Nohe A. Casein kinase 2 beta-subunit is a regulator of bone morphogenetic protein 2 signaling. *Biophys J*. 99(3):897–904. [PubMed: 20682268]
- Brown CM, Petersen NO. An image correlation analysis of the distribution of clathrin associated adaptor protein (AP-2) at the plasma membrane. *J Cell Sci*. 1998; 111 (Pt 2):271–281. [PubMed: 9405317]
- Chang H, Brown CW, Matzuk MM. Genetic analysis of the mammalian transforming growth factor-beta superfamily. *Endocr Rev*. 2002; 23(6):787–823. [PubMed: 12466190]
- Chiellini C, Cochet O, Negroni L, Samson M, Poggi M, Ailhaud G, Alessi MC, Dani C, Amri EZ. Characterization of human mesenchymal stem cell secretome at early steps of adipocyte and osteoblast differentiation. *BMC Mol Biol*. 2008; 9:26. [PubMed: 18302751]
- Crockett JC, Rogers MJ, Coxon FP, Hocking LJ, Helfrich MH. Bone remodelling at a glance. *J Cell Sci*. 2011; 124(Pt 7):991–998. [PubMed: 21402872]
- Di Guglielmo GM, Le Roy C, Goodfellow AF, Wrana JL. Distinct endocytic pathways regulate TGF-beta receptor signalling and turnover. *Nat Cell Biol*. 2003; 5(5):410–421. [PubMed: 12717440]
- Fujimoto T, Kogo H, Nomura R, Une T. Isoforms of caveolin-1 and caveolar structure. *J Cell Sci*. 2000; 113(Pt 19):3509–3517. [PubMed: 10984441]
- Hartung A, Bitton-Worms K, Rechtman MM, Wenzel V, Boergermann JH, Hassel S, Henis YI, Knaus P. Different routes of bone morphogenetic protein (BMP) receptor endocytosis influence BMP signaling. *Mol Cell Biol*. 2006; 26(20):7791–7805. [PubMed: 16923969]
- Hata K, Nishimura R, Ikeda F, Yamashita K, Matsubara T, Nokubi T, Yoneda T. Differential roles of Smad1 and p38 kinase in regulation of peroxisome proliferator-activating receptor gamma during bone morphogenetic protein 2-induced adipogenesis. *Mol Biol Cell*. 2003; 14(2):545–555. [PubMed: 12589053]
- Judex S, Donahue LR, Rubin C. Genetic predisposition to low bone mass is paralleled by an enhanced sensitivity to signals anabolic to the skeleton. *Faseb J*. 2002; 16(10):1280–1282. [PubMed: 12153999]
- Kamiya N, Ye L, Kobayashi T, Lucas DJ, Mochida Y, Yamauchi M, Kronenberg HM, Feng JQ, Mishina Y. Disruption of BMP signaling in osteoblasts through type IA receptor (BMPRIA) increases bone mass. *J Bone Miner Res*. 2008; 23(12):2007–2017. [PubMed: 18684091]
- Kaps C, Hoffmann A, Zilberman Y, Pelled G, Haupl T, Sittinger M, Burmester G, Gazit D, Gross G. Distinct roles of BMP receptors Type IA and IB in osteo-/chondrogenic differentiation in mesenchymal progenitors (C3H10T1/2). *Biofactors*. 2004; 20(2):71–84. [PubMed: 15322331]
- Lajoie P, Goetz JG, Dennis JW, Nabi IR. Lattices, rafts, and scaffolds: domain regulation of receptor signaling at the plasma membrane. *J Cell Biol*. 2009; 185(3):381–385. [PubMed: 19398762]
- Lee KS, Kim HJ, Li QL, Chi XZ, Ueta C, Komori T, Wozney JM, Kim EG, Choi JY, Ryoo HM, Bae SC. Runx2 is a common target of transforming growth factor beta1 and bone morphogenetic protein 2, and cooperation between Runx2 and Smad5 induces osteoblast-specific gene expression in the pluripotent mesenchymal precursor cell line C2C12. *Mol Cell Biol*. 2000; 20(23):8783–8792. [PubMed: 11073979]
- Mishina Y, Starbuck MW, Gentile MA, Fukuda T, Kasparcova V, Seedor JG, Hanks MC, Amling M, Pinero GJ, Harada S, Behringer RR. Bone morphogenetic protein type IA receptor signaling regulates postnatal osteoblast function and bone remodeling. *J Biol Chem*. 2004; 279(26):27560–27566. [PubMed: 15090551]
- Mishra L, Marshall B. Adaptor proteins and ubiquitinators in TGF-beta signaling. *Cytokine Growth Factor Rev*. 2006; 17(1–2):75–87. [PubMed: 16359909]
- Moerman EJ, Teng K, Lipschitz DA, Lecka-Czernik B. Aging activates adipogenic and suppresses osteogenic programs in mesenchymal marrow stroma/stem cells: the role of PPAR-gamma2

- transcription factor and TGF-beta/BMP signaling pathways. *Aging Cell*. 2004; 3(6):379–389. [PubMed: 15569355]
- Nakamura Y, Wakitani S, Nakayama J, Wakabayashi S, Horiuchi H, Takaoka K. Temporal and spatial expression profiles of BMP receptors and noggin during BMP-2-induced ectopic bone formation. *J Bone Miner Res*. 2003; 18(10):1854–1862. [PubMed: 14584896]
- Nohe A, Keating E, Fivaz M, van der Goot FG, Petersen NO. Dynamics of GPI-anchored proteins on the surface of living cells. *Nanomedicine*. 2006; 2(1):1–7. [PubMed: 17292110]
- Nohe A, Keating E, Knaus P, Petersen NO. Signal transduction of bone morphogenetic protein receptors. *Cell Signal*. 2004a; 16(3):291–299. [PubMed: 14687659]
- Nohe A, Keating E, Loh C, Underhill MT, Petersen NO. Caveolin-1 isoform reorganization studied by image correlation spectroscopy. *Faraday Discuss*. 2004b; 126:185–195. discussion 245–154. [PubMed: 14992406]
- Nohe A, Keating E, Underhill TM, Knaus P, Petersen NO. Effect of the distribution and clustering of the type I A BMP receptor (ALK3) with the type II BMP receptor on the activation of signalling pathways. *J Cell Sci*. 2003; 116(Pt 16):3277–3284. [PubMed: 12829744]
- Nohe A, Keating E, Underhill TM, Knaus P, Petersen NO. Dynamics and interaction of caveolin-1 isoforms with BMP-receptors. *J Cell Sci*. 2005; 118(Pt 3):643–650. [PubMed: 15657086]
- Nohe A, Petersen NO. Analyzing for co-localization of proteins at a cell membrane. *Curr Pharm Biotechnol*. 2004a; 5(2):213–220. [PubMed: 15078156]
- Nohe A, Petersen NO. Analyzing protein-protein interactions in cell membranes. *Bioessays*. 2004b; 26(2):196–203. [PubMed: 14745838]
- Nohe A, Petersen NO. Image correlation spectroscopy. *Sci STKE*. 2007; (417):pl7. [PubMed: 18089858]
- Ovchinnikov DA, Selever J, Wang Y, Chen YT, Mishina Y, Martin JF, Behringer RR. BMP receptor type IA in limb bud mesenchyme regulates distal outgrowth and patterning. *Dev Biol*. 2006; 295(1):103–115. [PubMed: 16630606]
- Ponce ML, Koelling S, Kluever A, Heinemann DE, Miosge N, Wulf G, Frosch KH, Schutze N, Hufner M, Siggelkow H. Coexpression of osteogenic and adipogenic differentiation markers in selected subpopulations of primary human mesenchymal progenitor cells. *J Cell Biochem*. 2008; 104(4):1342–1355. [PubMed: 18286543]
- Razani B, Zhang XL, Bitzer M, von Gersdorff G, Bottinger EP, Lisanti MP. Caveolin-1 regulates transforming growth factor (TGF)-beta/SMAD signaling through an interaction with the TGF-beta type I receptor. *J Biol Chem*. 2001; 276(9):6727–6738. [PubMed: 11102446]
- Semrau S, Schmidt T. Membrane heterogeneity -from lipid domains to curvature effects. *Soft Matter*. 2009; 5(17):3174–3186.
- Sieczkarski SB, Whittaker GR. Dissecting virus entry via endocytosis. *J Gen Virol*. 2002; 83(Pt 7):1535–1545. [PubMed: 12075072]
- Skillington J, Choy L, Derynck R. Bone morphogenetic protein and retinoic acid signaling cooperate to induce osteoblast differentiation of preadipocytes. *J Cell Biol*. 2002; 159(1):135–146. [PubMed: 12379805]
- Sottile V, Seuwen K. Bone morphogenetic protein-2 stimulates adipogenic differentiation of mesenchymal precursor cells in synergy with BRL 49653 (rosiglitazone). *FEBS Lett*. 2000; 475(3):201–204. [PubMed: 10869556]
- Thomas CM, Smart EJ. Caveolae structure and function. *J Cell Mol Med*. 2008; 12(3):796–809. [PubMed: 18315571]
- Tsuji K, Bandyopadhyay A, Harfe BD, Cox K, Kakar S, Gerstenfeld L, Einhorn T, Tabin CJ, Rosen V. BMP2 activity, although dispensable for bone formation, is required for the initiation of fracture healing. *Nat Genet*. 2006; 38(12):1424–1429. [PubMed: 17099713]
- Wang A, Ding X, Sheng S, Yao Z. Bone morphogenetic protein receptor in the osteogenic differentiation of rat bone marrow stromal cells. *Yonsei Med J*. 2010; 51(5):740–745. [PubMed: 20635450]
- Yeh LC, Unda R, Lee JC. Osteogenic protein-1 differentially regulates the mRNA expression of bone morphogenetic proteins and their receptors in primary cultures of osteoblasts. *J Cell Physiol*. 2000; 185(1):87–97. [PubMed: 10942522]

Zhang YW, Yasui N, Ito K, Huang G, Fujii M, Hanai J, Nogami H, Ochi T, Miyazono K, Ito Y. A RUNX2/PEBP2alpha A/CBFA1 mutation displaying impaired transactivation and Smad interaction in cleidocranial dysplasia. Proc Natl Acad Sci U S A. 2000; 97(19):10549–10554. [PubMed: 10962029]

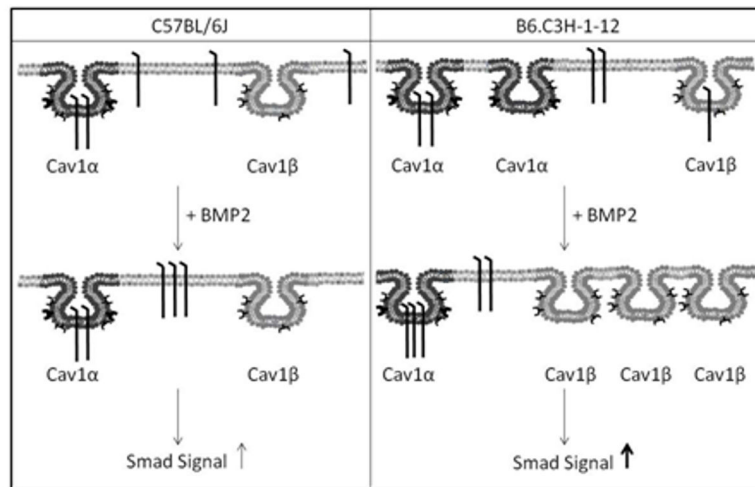


Figure 1. Summary of BMP2-induced BMPRIa and caveolae dynamics

The left panel is the summary from the BMSCs data isolated from the C57BL/6J. BMPRIa is localized to caveolae enriched with Cav1 α , while some receptors are not localized to caveolae (located at the cell surface). The addition of BMP2 decreased CD for BMPRIa. No change was observed for caveolae. The amount of BMPRIa localized to caveolae enriched with Cav1 α did not significantly change in the C57BL/6J. These dynamics led to increased Smad signaling. The right panel shows the summary from the BMSCs isolated from the B6.C3H-1-12. BMPRIa is localized to the cell surface, Cav1 α and Cav1 β enriched caveolae. BMP2 stimulation led to increased CD for caveolae resulting in increased Cav1 β enriched caveolae and decreased Cav1 α enriched caveolae. There was no change with the CD for BMPRIa. BMPRIa in Cav1 β enriched caveolae domains shuttled to Cav1 α caveolae in response to BMP2. This led to increased Smad signaling, more so than C57BL/6J.

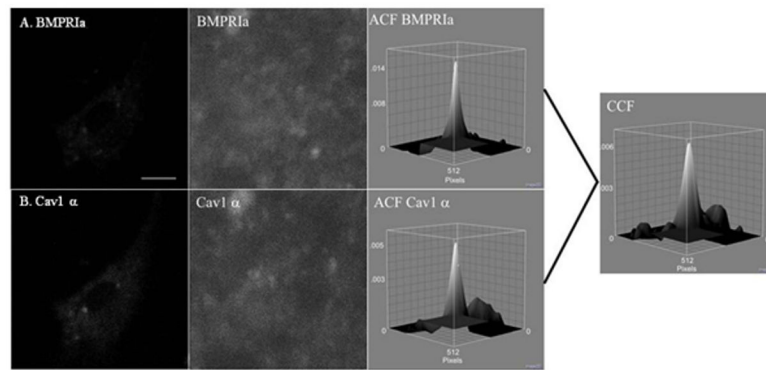


Figure 2. Auto and Cross Correlation Functions of BMPRIa and Cav1 α in C57BL/6J BMSCs were isolated and cultured on glass cover slips. The proteins, BMPRIa and Cav1 α , were labeled with a primary followed by a fluorescent secondary antibody. Images were taken at high resolution of the cellular membrane. Following confocal microscopy ICS and ICCS was performed on the images. A sample image of BMSC isolated from the C57BL/6J labeled for A) BMPRIa and B) Cav1 α with the corresponding high resolution image and auto correlation function. The cross correlation function for ICCS is to the right for the image.

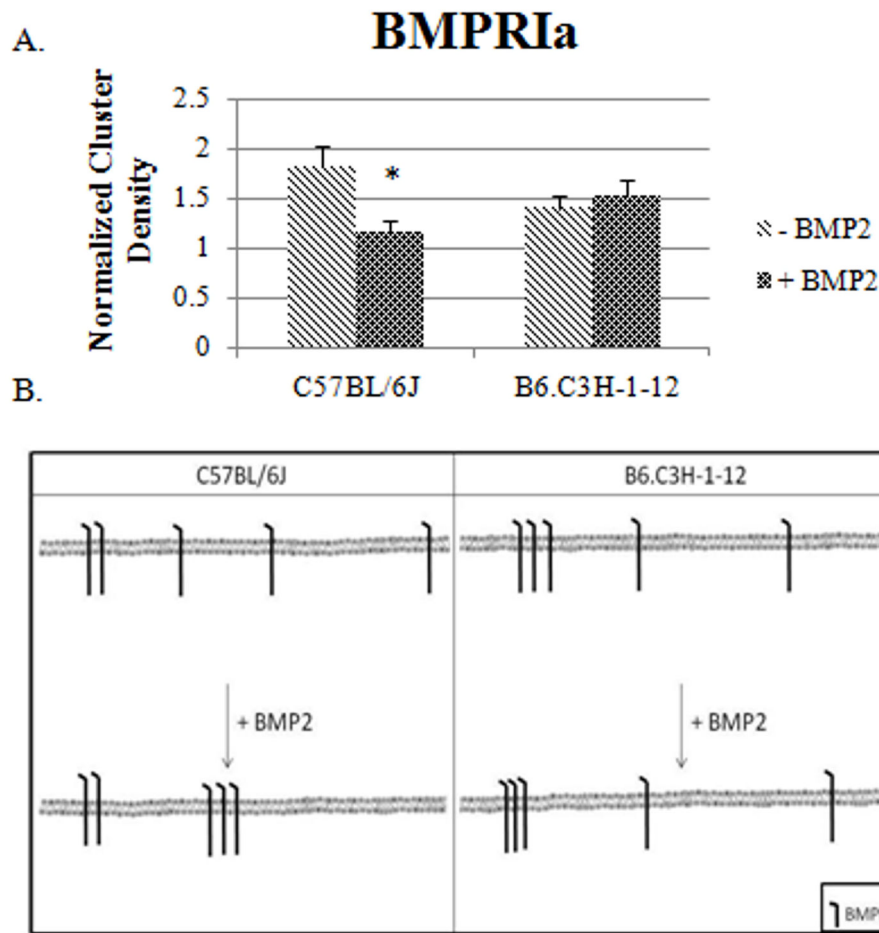


Figure 3. BMP2 stimulation led to a decrease in the clustering of BMPRIa on the cell surface of BMSCs isolated from C57BL/6J mice and no change for B6.C3H-1-12 mice
 BMSCs were isolated from 8 week old female C57BL/6J and B6.C3H-1-12 mice and stimulated or not stimulated with BMP2 (40nM). Cells were fixed using acetone/methanol and labelled for BMPRIa using a polyclonal goat BMPRIa antibody (Santa Cruz) followed by a secondary donkey anti goat Alexa 546 (molecular probes). High magnification images of flat regions of the plasma membrane were collected using a confocal microscope and the CD of BMPRIa was calculated. A) In the C57BL/6J the CD decreased with BMP2 stimulation. There was no change in CD in B6.C3H-1-12 mice with BMP2 stimulation. B) The summary of the CD results for BMSCs isolated from the C57BL/6J and B6.C3H-1-12.* Indicates significance as detected by one tailed student t test ($p < 0.05$).

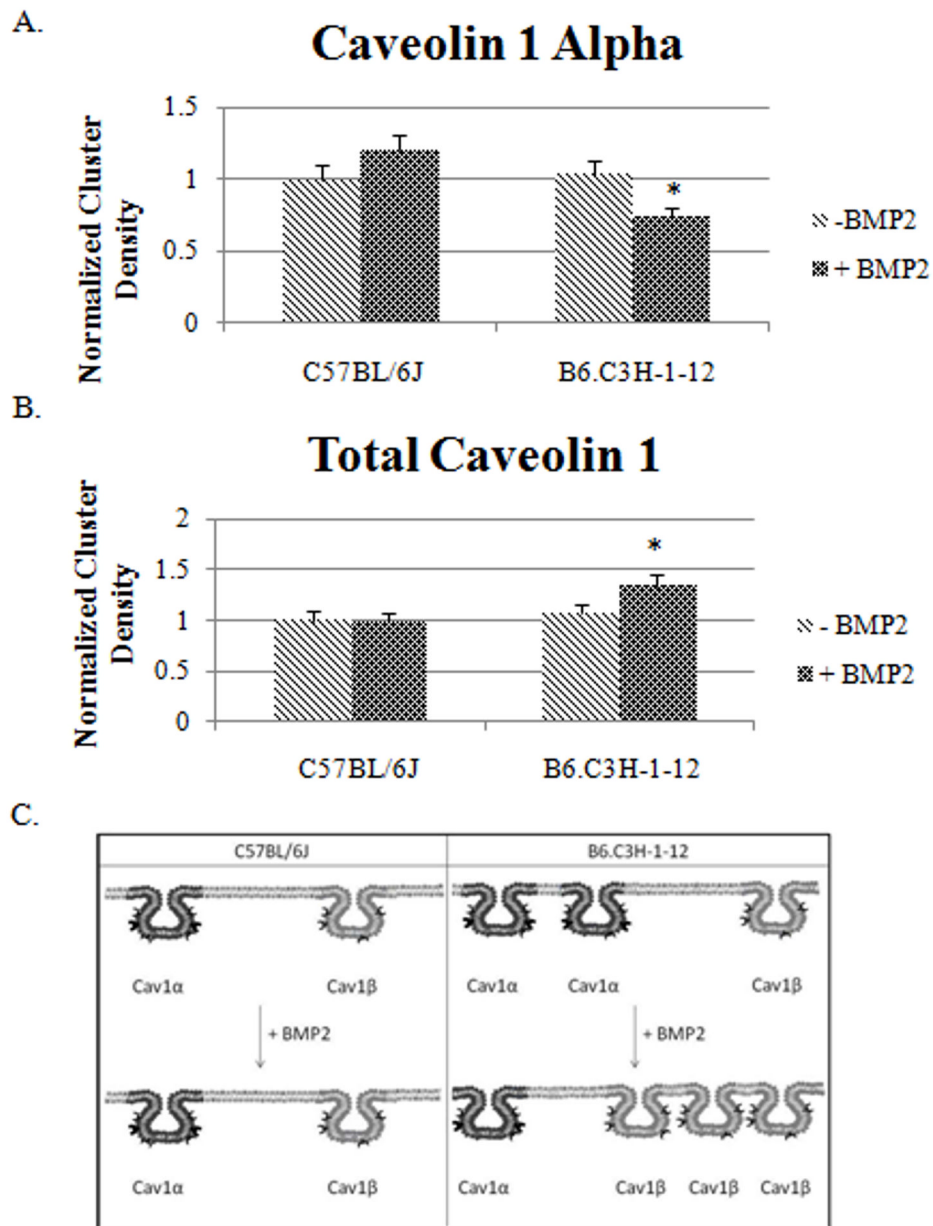


Figure 4. BMP2 stimulation leads to Caveolin-1 dispersion in BMSCs isolated from B6.C3H-1-12 mice

A and B) BMSCs were isolated from 8 week old female mice. 1×10^{-5} cells were plated on a 25mm round cover slip. After 10 days cells were stimulated or not stimulated with BMP2 (40nM). After fixation with acetone/methanol, cells were fluorescently labeled for B) Cav1 α or C) Cav1 Total. Forty high magnification images were collected and ICS analysis was performed. The Cluster Density (CD), which is the average number of clusters per unit area, was calculated. BMP2 stimulation led to a no significant change in the CD of labeled Cav1 α or Cav1 total of the C57BL/6J. Stimulation of BMP2 led to a significant decrease in labeled Cav1 α caveolae and an increased in labeled Cav1 total in BMSCs isolated from B6.C3H-1-12 mice ($p < 0.05$). C) The summary of the CD results for Cav1 total and Cav1 α in the BMSCs isolated from the C57BL/6J and B6.C3H-1-12. * Indicates significance with one tail student t test.

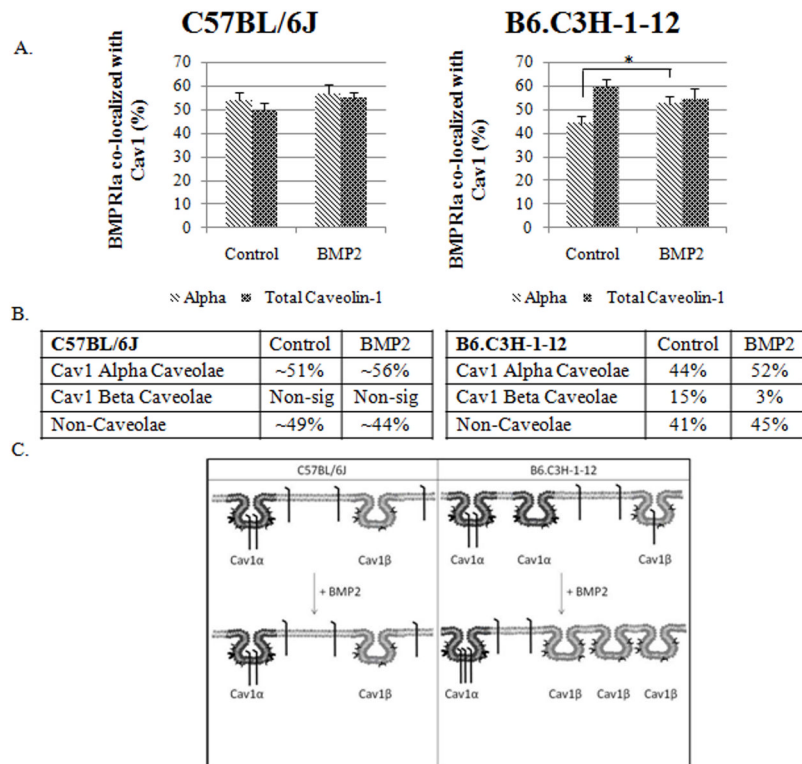


Figure 5. BMPRIa co-localized to a higher extent with caveolae in BMSCs isolated from B6.C3H-1-12 mice C57BL/6J

BMSCs isolated from B6.C3H-1-12 and C57BL/6J mice were stimulated after 10 days in culture with BMP2 or not as indicated. Cells were fixed and stained for BMPRIa and Cav1 isoforms as indicated. High magnification images were collected and the percent of co-localization was calculated using Image Cross Correlation Spectroscopy. The top panel shows the graphs of ICCS data collected. In BMSCs of the C57BL/6J mice (left side), ~51% and ~56% of BMPRIa co-localized with labelled Cav1 α and Cav1 total respectively. BMP2 stimulation led to a no significant change in co-localization. B6.C3H-1-12 (right side) mice showed 44% and 52% of BMPRIa co-localized with labelled Cav1 α and Cav1 total. Stimulation with BMP2 led to a significance increase to 52% for labelled Cav1 α . There was no significant change in the co-localization for labelled Cav1 total. The middle panel shows tables of the calculated percentages of co-localization of BMPRIa with Cav1 α or Cav1 β enriched caveolae. Since the percentage of BMPRIa co-localized with labelled Cav1 α and Cav1 total were very similar (overlapping error bars) these numbers were averaged for the table. The lower panel shows the overall trends that were observed for BMPRIa co-localization with caveolae. * Indicates significance as detected by one tailed student t test ($p < 0.05$).

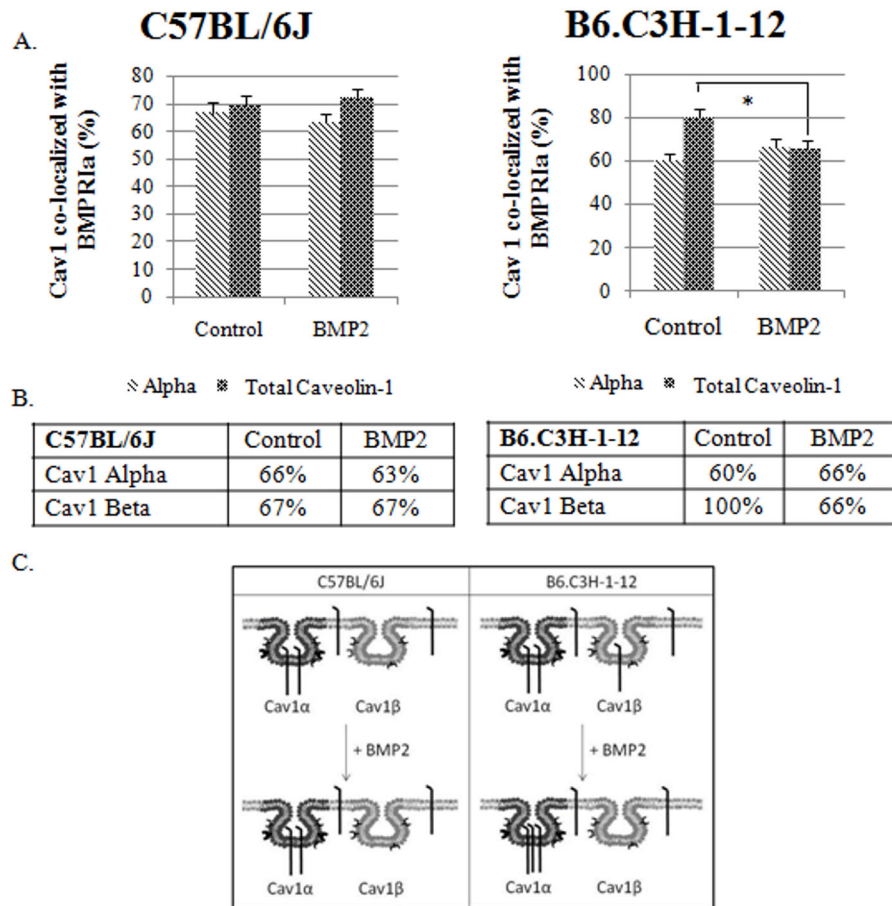


Figure 6. BMP2 led to a decrease of Cav1 co-localization with BMPRIa in BMSCs isolated from B6.C3H-1-12 mice

BMSCs isolated from 8 week old female C57BL/6J (left) or B6.C3H-1-12 (right) mice were fixed and stained for BMPRIa and Cav1 isoforms. The top panel illustrates the ICCS graphs. In BMSCs isolated from C57BL/6J, ~67% of the Cav1 α and ~67% of Cav1 total co-localized with BMPRIa. Upon BMP2 stimulation there was no significant change in the co-localization for both labelled Cav1 α and Cav1 total. In the B6.C3H-1-12, there was no significant change in the co-localization of labelled Cav1 α with BMPRIa. In the absence of BMP2 80% of labelled Cav1 total co-localized with BMPRIa, with BMP2 stimulation there was a significant decrease (66%) in co-localization. The middle panel shows a table of calculated percentages of co-localization between Cav1 and BMPRIa. The lower panel is the overall trends that were observed from the graph of Cav1 co-localization with BMPRIa. * Indicates significance as detected by one-tailed student t test ($p < 0.05$).

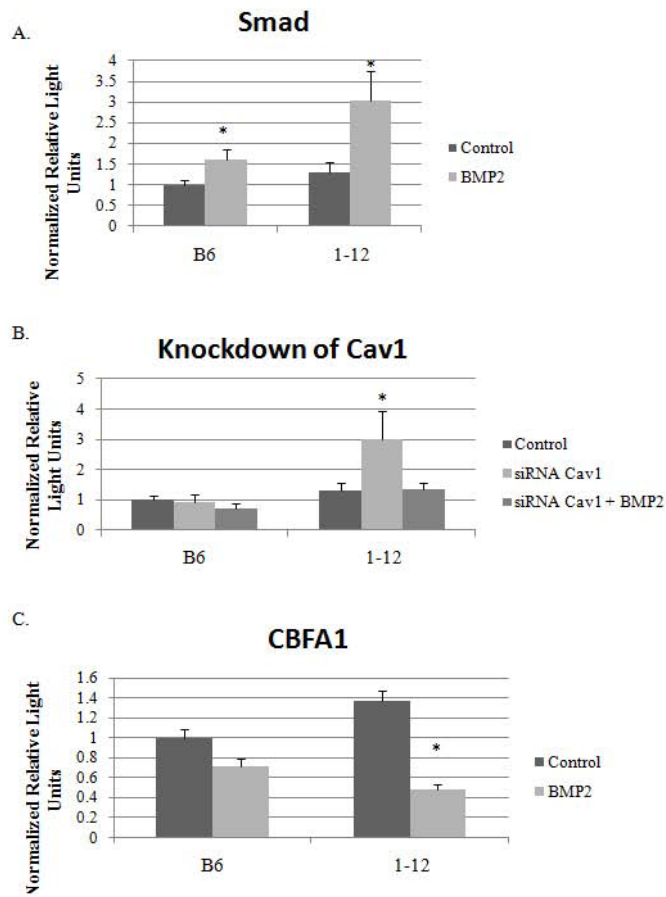


Figure 7. Increased Smad and Cbfa1 pathways are activated in the B6.C3H-1-12 mice BMSCs isolated from C57BL/6J and B6.C3H-1-12 female mice were transfected with A) pSBE, B) pSBE and siRNA for Cav1, C) CBFA1, and with a plasmid encoding renilla (pRL-luc) for normalization. After four hours cells were then stimulated or not with BMP2 (40nM). Reporter gene assays were performed 12 hours later. A) In the C57BL/6J and B6.C3H-1-12 there was an increase in Smad signalling with BMP2 stimulation. B) The knockdown of Cav1 induced Smad signalling independent of BMP2 in BMSCs from B6.C3H-1-12. Both C57BL/6J and B6.C3H-1-12, the knockdown of Cav1 blocked BMP2-induced Smad signalling. C) The basal level of Cbfa1 is increased in cells from B6.C3H-1-12 compared to C57BL/6J. The addition of BMP2 showed a trend of decreased signaling in C57BL/6J and significant decrease in B6.C3H-1-12. * Indicates significance as detected by student t test for A) and C), ANOVA followed by Tukey's test for B) ($p < 0.05$).

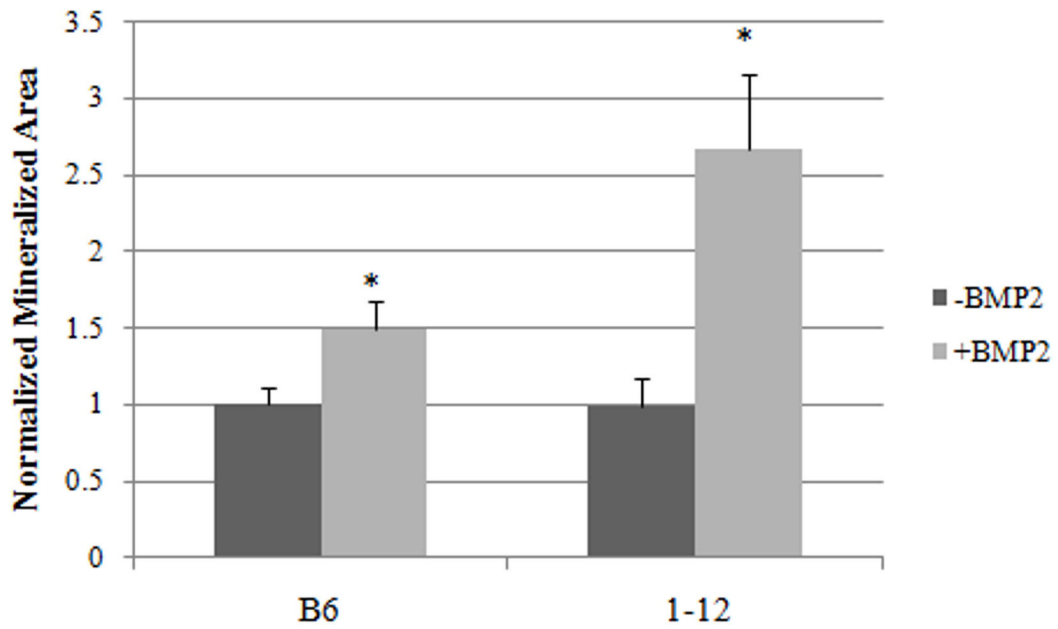


Figure 8. There is increased mineralization induced by BMP2 in the B6.C3H-1-12 mice BMSCs isolated from the C57BL/6J and B6.C3H-1-12 female mice were cultured in 24 well plates for 10 days. Cells were treated with BMP2 (40nM) or left non-stimulated to serve as controls. After 12 days cells were stained for mineralization with von Kossa. BMP2 stimulation significantly increased mineralization by BMSCs isolated from the C57BL/6J and B6.C3H-1-12. BMP2 treatments were normalized to corresponding control. * Indicates significance as detected by student t test ($p < 0.05$).